Dynamic resistance measurements in a GdBCO-coated conductor

Zhenan Jiang, Ryuki Toyomoto, Naoyuki Amemiya, Chris W. Bumby, Rodney A. Badcock, Nicholas J. Long

***Abstract*— Dynamic resistance is a phenomenon which occurs when a superconducting wire carries DC transport current whilst experiencing an alternating magnetic field. This situation occurs in a range of HTS machinery applications, where dynamic resistance can lead to large parasitic heat loads and potential quench events. Here, we present dynamic resistance measurements of a 5 mm-wide Fujikura coated conductor wire at 77 K. We report experimental values obtain through varying the field angle (the angle between magnetic field and normal vector of the conductor wide-face), the DC current levels, and the magnetic field amplitude, and frequency. We show that the dynamic resistance in perpendicular magnetic field can be predicted using a simple analytical equation. We also show that, across the range of field angles measured here the dynamic resistance is dominated by the perpendicular component of the applied magnetic field.**

***Index Terms*— Dynamic resistance, ReBCO, GdBCO, coated conductor.**

I. Introduction

Dynamic resistance occurs when a superconducting wire carries DC transport current whilst experiencing an alternating magnetic field [1, 2]. In HTS applications such as rotating machines, magnets, and SMES (Superconducting Energy Storage Systems), dynamic resistance plays an important role [3-6]. In HTS flux pumps, dynamic resistance within the HTS stator determines the maximum available output current [7-11]. In recent years, HTS coated conductors have become the dominant wire choice for next generation superconducting machines [12], and hence accurate prediction of the dynamic resistance incurred within an HTS coated conductor wire is a critical issue.

Oomen *et al* developed an analytical model for calculating dynamic resistance in a superconducting slab in an AC parallel magnetic field [2]. There have been some previous experimental reports on dynamic resistance in coated conductors in AC perpendicular magnetic fields [13, 14]. However, this previous work has only employed applied magnetic field amplitudes of < 20 mT, and the wire I_c value for the measurements reported in [13] was much smaller than today's wires.

Recently we have measured the dynamic resistance in a 4 mm-wide SuperPower coated conductor in AC perpendicular magnetic field up to 100 mT, and have developed an equation which can predict dynamic resistance in a superconducting strip in perpendicular magnetic field. This approach employs a formula adapted from the Oomen equation for a superconducting slab in parallel magnetic fields [15].

Here, we present dynamic resistance measurement results in a 5 mm-wide Fujikura GdBCO coated conductor at 77 K. This Fujikura wire has a considerably higher self-field I_c than the 4 mm-wide SuperPower wire previously reported, and hence provides a test of the useful applicability of our developed equation. In addition, in this work we examine the dependence of dynamic resistance on the applied field angle (the angle between magnetic field and normal vector of the conductor wide-face, α, see Fig. 1).

FIG. 1 HERE

II. Experimental Method

Fig. 2(a) shows the experimental set-up used to make our dynamic resistance measurements at 77 K [16]. The AC magnet can generate up to 100 mT peak magnetic field at frequencies up to 112.5 Hz. The sample can be rotated inside the magnet, and the field angle, α can be varied from 0° to 360°. A 300 A DC power supply was used to supply DC current to the 15 cm-long Fujikura sample wire (FYSC-SC05). The sample was fabricated by IBAD/PLD method, and has a self-field I_c of 266.0 A at the 1 μV/cm criterion, 77 K. The specification of the sample is shown in Table 1. The DC circuit was arranged in order to reduce coupling with the AC magnet circuit. Fig. 2(b) shows voltage taps attached on the sample. Two sets of voltage taps were prepared as seen in Fig. 2(b): in the first set, two voltage taps were attached on the center of the sample, and two voltage signal wires run opposite along the sample axis and meet in the center of the sample; in the second set, a spiral loop was arranged around the sample as shown in the figure [17]. The spiral loop was introduced to cancel out the effect from external magnetic field. The distance between the voltage-taps is 5 cm. The voltage output from the voltage taps were measured using a Keithley 2182 nano-voltage meter. Appropriate filters were used to average the voltage from the voltage taps [18]. Dynamic resistance values measured from the two voltage pick-ups were exactly the same, and the first set of

Manuscript submitted September 02, 2016. This work was partially supported by the JSPS (Japan Society for the Promotion of Science).

Zhenan Jiang, Chris W. Bumby, Rodney A. Badcock, and Nicholas J. Long are with the Robinson Research Institute, Victoria University of Wellington, PO Box 33436, Lower Hutt 5046, New Zealand. (e-mail: zhenan.jiang@vuw.ac.nz).

Ryuki Toyomoto and Naoyuki Amemiya are with Graduate School of Engineering, Kyoto University, Kyoto, Kyoto-Daigaku-Katsura, Nishikyo, Kyoto 615-8510, Japan.

voltage taps was used in this work.

FIG. 2 HERE
TABLE 1 HERE

III. Equation for Dynamic Resistance in a Strip in Perpendicular Magnetic Field

The dynamic resistance per unit length per cycle in a superconducting strip, carrying DC current exposed to AC perpendicular magnetic field, $R_{d,\perp}$, can be estimated using the following equation [15],

$$\frac{R_{d,\perp}}{fL} = \frac{4a}{I_{c0}}\left(B_{a,\perp} - B_{th,\perp}\right) \qquad (1)$$

where a is half-width of the coated conductor, $B_{a,\perp}$ is the amplitude of applied magnetic field, I_{c0} (266.0 A) is the self-field critical current of the conductor, I_t is the DC transport current, f is the frequency of the applied magnetic field, L is the distance between the two voltage taps. The threshold magnetic field, $B_{th,\perp}$ is given by,

$$B_{th,\perp} = B_{p,\perp}\left(1 - \frac{I_t}{I_{c0}}\right) \qquad (2)$$

where $(1- I_t/I_{c0})$ is the DC current filling factor and $B_{p,\perp}$ is effective penetration field [19, 20], which can be evaluated by finding B_a value at the maxima of the Γ curve shown in Fig. 3. In this figure $\Gamma = Q_{BI}/B_a^2$, where Q_{BI} is the Brandt expression for the theoretical magnetization loss in a superconducting strip exposed to AC perpendicular magnetic field [21]. The maxima of this curve can be obtained from straightforward numerical methods to yield [15],

$$B_{p,\perp} = 4.9284\mu_0 J_{c0} t/\pi \qquad (3)$$

where J_{c0} is defined as $I_{c0}/(2a \times 2t)$. For the wire considered here, we calculate that $B_{p,\perp}$ =51.71 mT, as shown in Fig. 3.

FIG. 3 HERE

IV. Experimental Results

Fig. 4 shows the measured $R_{d,\perp}$ data obtained from the sample at 3 different frequencies and 4 different values of the reduced current, I_t/I_{c0}. In these plots $R_{d,\perp}$ is normalized by f. The $R_{d,\perp}$ data for different frequencies show close agreement, which indicates the hysteretic nature of the dynamic loss mechanism. In all plots, $R_{d,\perp}$ is zero until the threshold magnetic field, $B_{th,\perp}$, is exceeded. We have obtained experimental values for $B_{th,\perp}$ from the x-axis intercept of linear fits of the composite dataset using all frequencies measured for each value of I_t/I_{c0}. $B_{th,\perp}$ values decrease as the reduced current, I_t/I_{c0} is increased which is consistent with Eq. (2). In Fig. 4(d), the $R_{d,\perp}$ data for f = 26.62 Hz deviate from the linear fit. We believe this is due to flux flow loss which occurs as the $I_c(B)$ of the wire at the peak applied field falls below the magnitude of the total driven DC current [15]. Flux flow loss leads to a rapid increase in total dissipated power with increasing field amplitude, and we burnt out a sample during the measurement at I_t/I_{c0} = 0.9 and high B_a due to this effect.

FIG. 4 HERE

The experimentally derived values of $B_{th,\perp}$ from the Fujikura sample are shown in Fig. 5(a) alongside calculated values based on Eq. (2) [15]. The figure also shows calculated values obtained using an alternative formula proposed by Ciszek *et al*, which uses B_{th} values in parallel fields in conjunction with a calculated demagnetization factor [13]. It can be seen that the experimentally obtained values of $B_{th,\perp}$ have excellent agreement with the values determined using Eq. (2), while the Ciszek model only converges with our model and experiment at high I_t/I_{c0} values.

Fig. 5(b) compares the gradient of the linear fits (dR_d/dB_a) in Fig. 4 and the theoretical value of $4a/I_{c0}$ expected from Eq. (1). This is plotted as a function of the reduced current I_t/I_{c0}. In all cases the experimentally obtained gradient is larger than the theoretical value, although agreement improves slightly with increasing I_t/I_{c0}. The difference ranges between 30 – 15 %. There are several possible causes for this discrepancy, including: possible non-uniform J_c distributions in the sample wire; possible contributions due to J_c-B dependence of the wire; or possible errors in measured I_{c0} values and GDBCO film dimensions used in the theoretical calculations.

In Fig. 6, R_d data is plotted for measurements made at 3 different field angles, α = 0°, 30°, 60° , using 3 different I_t/I_{c0} values at 26.62 Hz. For a given I_t/I_{c0}, B_{th} increases with increasing field angle α while the gradient of the fitted linear lines, dR_d/dB_a, and decreases with increasing field angle α. These results can be explained by the fact that calculated dynamic resistance in parallel magnetic field [2] is negligible compared to our experimental results. For example, if we consider B_a= 100 mT, I_t/I_{c0} = 0.3 and f = 26.62 Hz, we find that the experimentally measured R_d at α = 60° is 1.19 μΩ/m/Hz. This can be compared with a calculated value for the expected dynamic resistance in parallel field of from the Oomen model of $R_{d,\parallel} = 5.76 \times 10^{-4}$ μΩ/m/Hz which is a factor of about 2000 smaller than the measured value. Fig. 7 shows calculated values of $R_{d,\parallel}$ for parallel field amplitudes up to 100 mT, and it is clear that $R_{d,\parallel} \ll R_d$ throughout the experimental range reported here. In light of this observation, it is reasonable to consider whether the angular dependence of R_d (α) can be explained simply by the perpendicular component of B_a which varies according to $B_a \cdot \cos\alpha$. Fig. 8 shows plots of $B_a \cdot \cos\alpha$ versus R_d at α = 0°, 30°, 60°. It is readily apparent that this simple transformation leads to the data collapsing onto an approximately common curve for all angles.

FIG. 6 HERE
FIG. 7 HERE

The apparent perpendicular threshold field, $B_{th,\perp}$ (given by

the *x*-axis intercept) now closely agree for the datasets collected at each field angle. This is a result of the very high aspect ratio of the coated conductor wire, which ensures that shielding currents are restricted to flow only within the ~ 2.3 μm GdBCO film. This gives rise to a magnetization field which is always perpendicular to the tape, and hence shields only the perpendicular component of the applied field. This situation is markedly different to that previously observed for BSCCO wire [18], where the aspect ratio of the filamentary zone is normally more than 100 times the aspect ratio ($2a/2t$) of a ReBCO wire.

FIG. 8 HERE

Fig. 8 also shows that the gradient $dR_d/dB_{a\perp}$, is also approximately constant at α = 0°, 30° and 60°, although the agreement at the largest field angle studied is not perfect, and suggests the emergence of a further small contributing factor. Nonetheless, Figure 8 provides strong evidence that R_d (α) of the GdBCO coated conductor wire can be well described by considering solely the contribution of the perpendicular field component to Eq. (1).

V. Conclusion

We have measured dynamic resistance in a 5 mm-wide Fujikura GaBCO coated conductor at 77 K when exposed to AC external magnetic fields at various applied field angles and amplitudes up to 100 mT.

The threshold field, $B_{th,\perp}$ of the coated conductor in perpendicular field can be accurately predicted from the penetration field, $B_{p,\perp}$ identified from the maxima of the Brandt gamma curve, and the DC current filling factor (1- I_t /I_{c0}). The measured dynamic resistance, $R_{d,\perp}$ values in perpendicular magnetic field, have reasonable agreement with the values predicted from the Oomen equation for a superconducting slab using the $B_{th,\perp}$ values.

We have also shown that the dynamic resistance due to an a magnetic field applied at angles up to 60 degrees from the perpendicular field, can be accurately determined by considering solely the contribution due to the perpendicular field component. This situation is contrary to that previously reported for BSCCO wire, and arises due to the very high aspect ratio of the coated conductor wire, which restricts shielding currents to flow solely in the plane of the ReBCO film.

Acknowledgment

The authors acknowledge Drs. N. Strickland and S. Wimbush for I_c (B, α) measurements of the sample at 77 K.

References

[1] K. Ogasawara, K. Yasukochi, S. Nose, and H. Sekizawa, "Effective resistance of current-carrying superconducting wire in oscillating magnetic fields 1: Single core composite conductor," *Cryoginics*, vol. 16, pp. 33-38, Jan. 1976.

[2] M. P. Oomen, J. Rieger, M. Leghissa, B. ten Haken, and H. H. J. ten Kate, "Dynamic resistance in a slab-like superconductor with $J_c(B)$ dependence," *Supercond. Sci. Technol.*, vol. 12, pp. 382-387, 1999.

[3] S. S. Kalsi, *Applications of high temperature superconductors to electric power equipment* (IEEE Press, New Jersey, 2011) pp.96.

[4] P. J. Masson, D. S. Soban, E. Upton, J. E. Pienkos, and C. A. Luongo, "HTS motors in aircraft propulsion: design considerations", IEEE *Trans. Appl. Supercond.* vol. 15, pp. 2218 - 2221, 2005.

[5] P. N. Barnes, M. D. Sumption, and G. L. Rhoads, "Review of high power density superconducting generators: Present state and prospects for incorporating YBCO windings", *Cryogenics* vol. 45, pp. 670-686, 2005.

[6] E. Pardo, "Modeling of AC loss in coils made of thin tapes under DC bias current", *IEEE Trans. Appl. Supercond.* vol. 24, 2013, Art. ID 4700105.

[7] Z. Jiang, K. Hamilton, N. Amemiya, R. A. Badcock, and C. W. Bumby, "Dynamic resistance of a high-T_c superconducting flux pump," *Appl. Phys. Lett*, vol. 105, Sep. 2014, Art. ID 112601.

[8] Z. Jiang, C. W. Bumby, R. A. Badcock, H. J. Sung, N. J. Long, and N. Amemiya, "Impact of flux gap upon dynamic resistance of a rotating HTS flux pump," *Supercond. Sci. Technol.*, vol. 28, Sep. 2015, Art. ID 115008.

[9] J. Geng and T. A. Coombs, "Mechanism of a high-Tc superconducting flux pump: Using alternating magnetic field to trigger flux flow", *Appl. Phys. Lett.* vol. 107, 2015, Art. ID 142601.

[10] C. W. Bumby, Z. Jiang, J. G. Storey, A. E. Pantoja, R. A. Badcock, "Anomalous open-circuit voltage from a high-T_c superconductor dynamo", *Appl. Phys. Lett.* vol. 108, 2016, Art. ID 122601.

[11] C. W. Bumby, R. A. Badcock, H. J. Sung, K. M. Kim, Z. Jiang, A. E. Pantoja, P. Bernado, M. Park, and R. G. Buckley, "Development of a brushless HTS exciter for a 10 kW HTS synchronous generator", *Supercond. Sci. Technol.* vol. 29, 2016, Art. ID 024008.

[12] V. Selvamanickam, A. Guevara, Y. Zhang, I. Kesgin, Y. Xie, G. Carota, Y. Chen, J. Dackow, Y. Zhang, Y. Zuev, C. Cantoni, A. Goyal, J. Coulter, and L. Civale, "Enhanced and uniform in-field performance in long (Gd, Y)–Ba–Cu–O tapes with zirconium doping fabricated by metal–organic chemical vapor deposition" *Supercond. Sci. Technol.* vol. 23, 2010, Art. ID 014014.

[13] M. Ciszek, O. Tsukamoto, J. Ogawa, and D. Miyagi, "Energy losses in YBCO-123 coated conductors carrying transport current in perpendicular external magnetic field", *AIP Conf. Proc.* vol. 614, pp. 606-613, 2002.

[14] R. C. Duckworth, Y. F. Zhang, T. Ha, and M. J. Gouge "Dynamic resistance of YBCO-coated conductors in applied AC fields with DC transport currents and DC background fields," *IEEE Trans. Appl. Supercond.*, vol. 21, pp. 3251-3256, June 2011.

[15] Z. Jiang, R. Toyomoto, N. Amemiya, X. Zhang, and C. W. Bumby, "Dynamic resistance of a high-T_c superconducting strip in perpendicular magnetic field at 77 K", *2016 In Press, Supercond. Sci. Technol.*, https://doi.org/10.1088/1361-6668/aa54e5

[16] Z. Jiang and N. Amemiya, "An experimental method for total AC loss measurement of high T_c superconductors", *Supercond. Sci. Technol.* vol. 17, pp. 371- 379, 2004.

[17] S. Fukui, Y. Kitoh, T. Numata, O. Tsukamoto, J. Fujikami, and K. Hayashi, "Transport current AC losses of high-Tc superconducting tapes exposed to AC magnetic field", Advances in Cryogenic Engineering, vol. 44, pp. 723-730, 1998.

[18] M. Ciszek, H. G. Knoopers, J. J. Rabbers, B. ten Haken, and H. H. J. ten Kate, "Angular dependence of the dynamic resistance and its relation to the AC transport current loss in Bi-2223/Ag tape superconductors" *Supercond. Sci. Technol.* vol. 15, pp. 1275- 1280, 2002.

[19] M. Iwakuma, K. Toyota, M. Nigo, T. Kiss, K. Funaki, Y. Iijima, T. Saitoh, Y. Yamada, and Y. Shiohara, "AC loss properties of YBCO superconducting tapes fabricated by IBAD-PLD technique," *Physica C*, vol. 412-414, pp. 983-991, May 2004.

[20] A. Palau, T. Puig, X. Obradors, E. Pardo, C. Navau, A. Sanchez, A. Usoskin, H. C. Freyhardt, L. Fernández, B. Holzapfel, and R. Feenstra, "Simultaneous inductive determination of grain and intergrain critical current densities of $YBa_2Cu_3O_{7-x}$ coated conductors", *Appl. Phys. Lett.* vol. 84, pp. 230 - 232, 2004.

[21] E. H. Brandt and M. Indenbom, "Type-II-superconductor strip with current in a perpendicular magnetic field," *Phys. Rew. B*, vol. 48, pp. 12893-12906, Nov. 1993.

TABLE I
Sample Specifications

Critical current at self-field, 77 K (A)	266
Width of conductor (mm)	5.07
Ag layer (μm)	6.4
Thickness of YBCO layer (μm)	2.3
Sample length (mm)	150
Thickness of substrate (μm)	100
Thickness of stabilizing layer (μm)	100

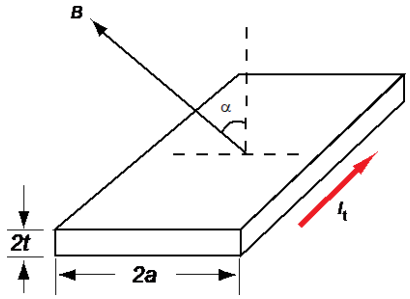

Fig. 1. Definition of field angle α.

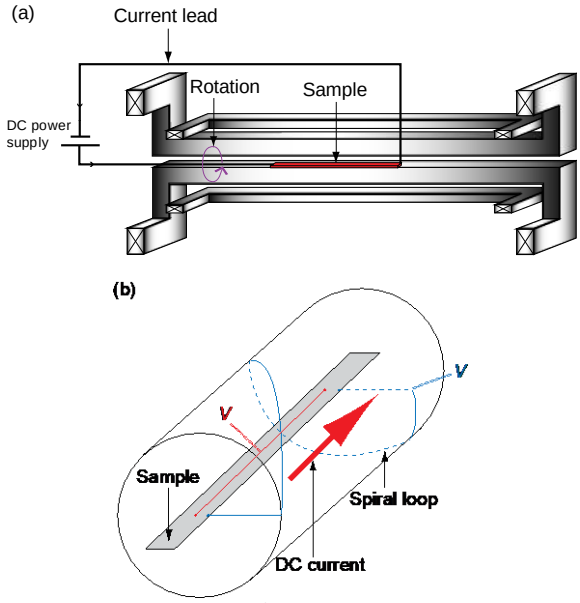

Fig. 2. (a) Experimental set-up for dynamic resistance measurement, (b) voltage tap arrangement.

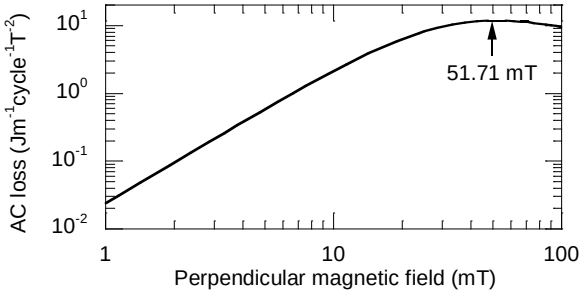

Fig. 3. Γ plot of calculated AC magnetization loss [21], $\Gamma = Q_{BI}/B_a^2$ used to define the effective penetration field, B_p in the sample. The maxima of Γ plot occurs when $B_a = B_p$, which in this work is found to be 51.71 mT.

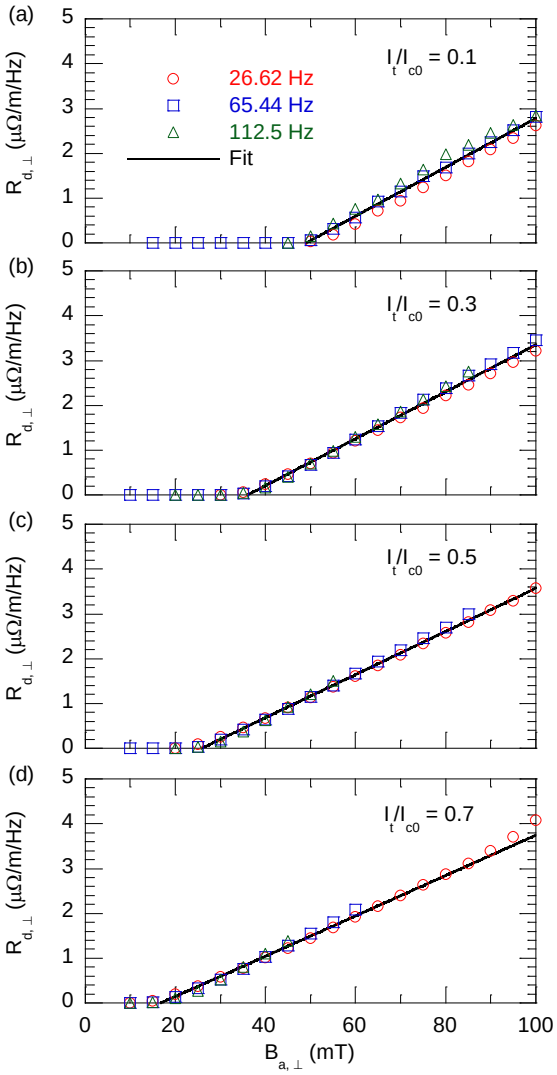

Fig. 4. Measured dynamic resistance values for different frequencies plotted as a function of the amplitude of the applied magnetic field (a) I_t/I_{c0} = 0.1, (b) I_t/I_{c0} = 0.3, (c) I_t/I_{c0} = 0.5, (d) I_t/I_{c0} = 0.7.

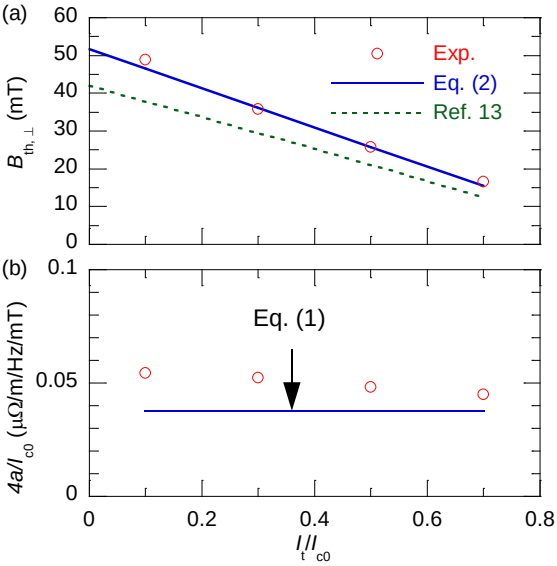

Fig. 5. (a) Threshold magnetic field in perpendicular magnetic field, $B_{th,\perp}$, vs. reduced current [15], (b) the gradient of the linear fits, dR_d/dB_a vs. $4a/I_{c0}$ from Eq. (1).

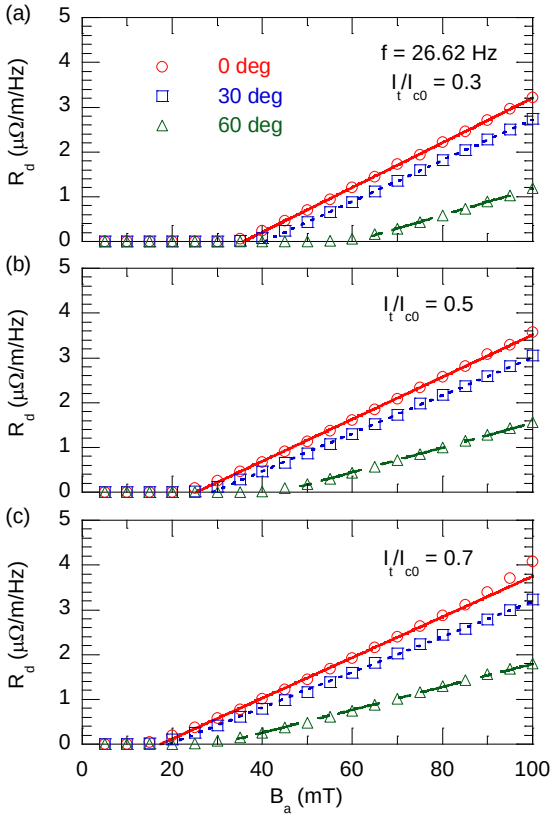

Fig. 6. Measured dynamic resistance in various field angles at 26.62 Hz, (a) $I_t/Ic_0 = 0.3$, (b) $I_t/Ic_0 = 0.5$, (c) $I_t/Ic_0 = 0.7$.

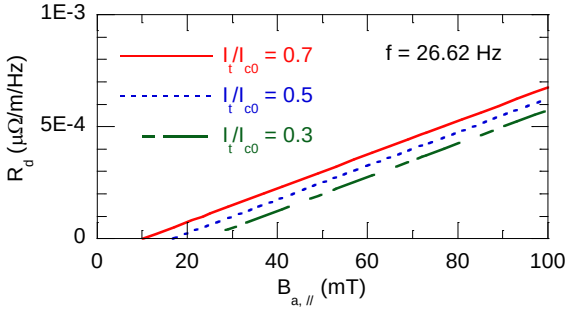

Fig. 7. Calculated dynamic resistance due to parallel magnetic field, $B_{a,//}$.

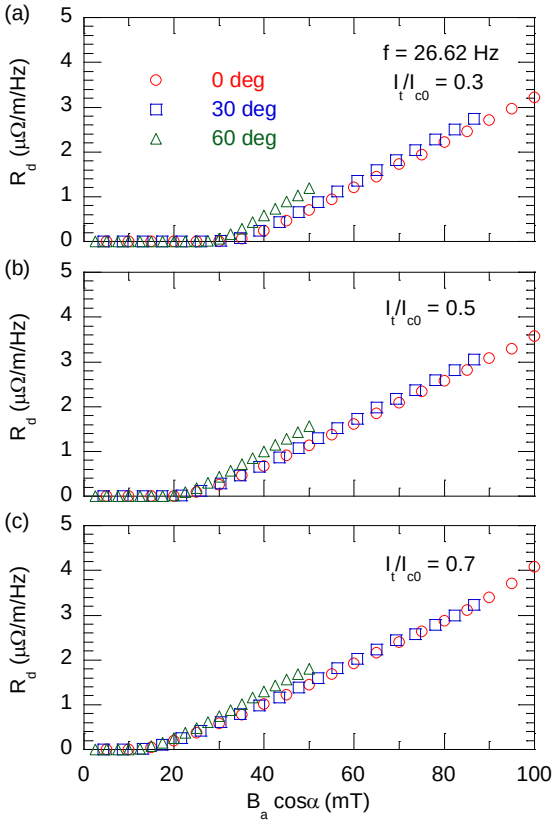

Fig. 8. Dynamic resistance in different field angles at 26.62 Hz, (a) $I_t/Ic_0 = 0.1$, (b) $I_t/Ic_0 = 0.3$, (c) $I_t/Ic_0 = 0.5$, (d) $I_t/Ic_0 = 0.7$.